

1 **Assessment of the fatality rate and transmissibility taking account of undetected cases**
2 **during an unprecedented COVID-19 surge in Taiwan**

3

4 **Hsiang-Yu Yuan^{1,2,*}, M. Pear Hossain¹, Tzai-Hung Wen³, Ming-Jiuh Wang⁴**

5

6 ¹ Department of Biomedical Sciences, Jockey Club College of Veterinary Medicine and Life
7 Sciences, City University of Hong Kong, Hong Kong SAR, China

8

9 ² Centre for Applied One Health Research and Policy Advice, City University of Hong Kong,
10 Hong Kong SAR, China

11

12 ³ Department of Geography, National Taiwan University, Taipei City, Taiwan

13 ⁴ Department of Anesthesiology, National Taiwan University Hospital, National Taiwan
14 University, Taiwan

15

16 *Correspondence to: Hsiang-Yu Yuan sean.yuan@cityu.edu.hk

17 Hsiang-Yu Yuan and M. Pear Hossain contributed equally to this article.

18

19

20

21 **Abstract**

22 Background

23 During the COVID-19 outbreak in Taiwan between May 11 and June 20, 2021, the observed
24 fatality rate (FR) was 5.3%, higher than the global average at 2.1%. The high number of
25 reported deaths suggests that hospital capacity was insufficient. However, many unexplained
26 deaths were subsequently identified as cases, indicating that there were a few undetected cases,
27 hence resulting in a higher estimate of FR. Estimating the number of total infected cases or
28 knowing how to reduce the undetected cases can allow an accurate estimation of the fatality
29 rate (FR) and effective reproduction number (R_t).

30 Methods

31 After adjusting for reporting delays, we estimated the number of undetected cases using
32 reported deaths that were and were not previously detected. The daily FR and R_t were
33 calculated using the number of total cases (i.e. including undetected cases). A logistic
34 regression model was developed to predict the detection ratio among deaths using selected
35 predictors from daily testing and tracing data.

36 Results

37 The estimated true daily case number at the peak of the outbreak on May 22 was 897, which
38 was 24.3% higher than the reported number, but the difference became less than 4% on June 9
39 and afterward. After taking account of undetected cases, our estimated mean FR (4.7%) was
40 still high but the daily rate showed a large decrease from 6.5% on May 19 to 2.8% on June 6.
41 R_t reached a maximum value of 6.4 on May 11, compared to 6.0 estimated using the reported
42 case number. The decreasing proportion of undetected cases was associated with the increases
43 in the ratio of the number of tests conducted to reported cases, and the proportion of cases that
44 are contact-traced before symptom onset.

45 Conclusions

46 Increasing testing capacity and tracing efficiency can lead to a reduction of hidden cases and
47 hence improvement in epidemiological parameter estimation.

48

49 Introduction

50 Knowing the actual number of coronavirus disease 2019 (COVID-19) cases throughout an
51 outbreak is critical to provide an accurate estimate of epidemiological parameters such as the
52 fatality rate (FR) and effective reproduction number (R_t). These parameters aid in making
53 proper public health decisions, assessing health care system performance, and predicting the
54 trend of COVID-19 spread. However, the number of undetected cases can be large and may
55 vary during an outbreak. Limited capacities for contact tracing and testing often result in
56 underestimation of true infections ^{1,2}. The proportion of undetected cases may reduce after such
57 capacities improve. Hence, estimating this constantly changing proportion of undetected cases
58 throughout an outbreak is important.

59 After several months of zero confirmed community-acquired cases, quarantine exemption for
60 flight crews, and super spreader events in tea parlors in Wanhua in Taipei in late April and
61 early May 2021, triggered a fresh wave of local spread of the Alpha variant ³. This resulted in
62 14,005 total reported cases between May 11 and June 20, 2021 ⁴. Approximately 5% of cases
63 resulted in death, which was a higher case fatality rate (CFR) compared to the global rate
64 (obtained by dividing the total number of deaths by the total number of cases worldwide),
65 which has been consistently below 2.5% since November 16, 2020 ⁵. Whether this high CFR
66 was mainly because of insufficient hospital capacity and treatment, or a massive proportion of
67 undetected cases was unknown.

68 Early in the outbreak, testing capacity was insufficient to cope with the rising cases among
69 initial transmission clusters. The daily number of new cases grew to more than 200 within a
70 week and continued to increase until reaching a plateau at the end of May 2021 (i.e., 596 cases
71 on average per day from May 22 to 28). Because of the emerging outbreak, Taiwan had been
72 under Level 2 alert since May 11, 2021 ⁶, followed by escalation to Level 3 restrictions on May
73 19, 2021 ⁷, under which people are required to wear masks outdoors, gatherings of more than
74 four people indoors and more than nine people outdoors are banned, and all schools are closed.
75 Social distancing measures reduced individual mobility ⁸ and effectively lowered R_t . At the
76 same time, the daily number of tests conducted continued to increase, presumably allowing
77 more cases to be identified.

78 During the outbreak, many confirmed cases failed to be detected when alive but were tested
79 because of their death, indicating that a certain number of undetected cases existed. The number
80 of undetected cases who eventually died (referred to as **undetected deaths**), together with the

81 number of deaths who were known to have COVID-19 (referred to as **detected deaths**), can
82 be used to infer the proportion of undetected cases if their fatality rates are known. Presumably,
83 the probability of death among undetected cases is similar to that among detected cases during
84 the early period of the outbreak when hospital capacity and treatment is not sufficient.

85 Although knowing the numbers of detected and undetected deaths helps to estimate the
86 proportion of undetected cases and hence to guide interventions, a challenge exists that many
87 deaths from infection usually happen several weeks after symptom onset. This highlights the
88 importance of early estimation of the true number of total cases without delay. Hence, it is
89 important to know whether the changes in the proportion of detected deaths can be predicted
90 by daily testing and tracing data.

91 We quantified time-varying FR and R_t by taking into account the proportion of undetected
92 cases estimated using death data. We then developed a model based on logistic regression to
93 predict the proportion of undetected cases using daily data related to testing and tracing
94 capacity.

95 **Methods**

96 ***Data sources***

97 We collected the date of symptom onset time and testing date for each reported death of
98 COVID-19 from May 28 to July 22, 2021 from Taiwan Centers for Disease Control ⁹. The
99 daily number of deaths reported before May 28 was obtained from the media. Daily number of
100 confirmed cases was collected from Taiwan National Infectious Disease Statistics System ⁴.
101 We collected the daily number of tests conducted from the Government Information Open
102 Platform, Taiwan ^{10,11}.

103 ***Estimating true total cases and fatality rate***

104 Deaths from COVID-19 were classified into two categories, detected and undetected deaths,
105 depending on whether testing was performed before the death or not, respectively (see the
106 schema in Figure 1A). To estimate the number of true total cases, we first considered the
107 following ratio of undetected to detected deaths using the numbers of detected and undetected
108 cases and their respective FR:

$$109 \quad \frac{d_{ud}(t)}{d_d(t)} = \frac{c_{ud}(t) \times FR_{ud}}{c_d(t) \times FR_d(t)} \quad (1)$$

110 where d_d refers to the number of detected deaths, while d_{ud} refers to the number of undetected
111 deaths; $c_d(t)$ and $c_{ud}(t)$ represent the number of cases that are detected and undetected at day
112 t , respectively. Note that t refers to the reporting date for detected cases or detected deaths;
113 For undetected cases or undetected deaths, t refers to the adjusted reporting date such that the
114 reporting delay (i.e., the time elapsed between symptom onset and reporting) is adjusted to be
115 the same as that of detected cases. Thus, $d_d(t)$ represents the number of deaths among the
116 detected cases who are reported at day t . Similarly, $d_{ud}(t)$ is the number of deaths among the
117 undetected cases whose adjusted reporting date is at day t . $FR_d(t)$, which is likely to be
118 affected by the change in hospital capacity or treatment, represents the daily FR among the
119 detected cases at day t . FR_{ud} represents the FR among the undetected cases. FR_{ud} was
120 assumed to be a constant, estimated as the average $FR_d(t)$ during the initial two weeks (from
121 May 11 to May 24) of the outbreak when the hospital capacity or treatment was not sufficient.
122 Undetected deaths who are tested later are identified as “late-detected” cases (c_{ld}) (See Figure
123 1A). We back-projected the number of late-detected cases from their late reporting time to their
124 adjusted reporting date t ¹², using the mean and standard deviation of the reporting delay

125 among detected cases. Our aim was to estimate $c_{ud}(t)$. After rearrangement, the following
126 formula was derived:

$$127 \quad c_{ud}(t) = c_d(t) \times \frac{FR_d(t)}{FR_{ud}} / \frac{d_d(t)}{d_{ud}(t)} \quad (2)$$

128 The value can be solved because all of the terms on the right are either known or can be
129 estimated. We assumed that most of the undetected deaths were identified as “late-detected”
130 cases (c_{ld}). Therefore, the number of undetected deaths was approximated by the number of
131 late-detected cases ($d_{ud} \approx c_{ld}$) and then the ratio $\frac{d_d(t)}{d_{ud}(t)}$ was obtained. At the same time, the
132 proportion of detected deaths (i.e., the detection ratio among death cases; $\frac{d_d(t)}{d_d(t)+d_{ud}(t)}$) was also
133 calculated. Finally, the true number of total cases was derived empirically as the sum of
134 detected and undetected cases (i.e., $c_d + c_{ud}$). Note that these ratios among deaths were also
135 predicted by a regression model using data related to testing and tracing and hence a model-
136 predicted number of total cases was obtained (see later sections).

137 The FRs of reported cases (including both detected and late-detected cases; $c_d + c_{ld}$) and total
138 cases were estimated at the reporting time (or the adjusted reporting time for undetected cases)
139 using the following equations.

$$140 \quad FR_{reported}(t) = \left(\frac{d_d(t) + c_{ld}(t)}{c_d(t) + c_{ld}(t)} \right) \quad (3)$$

$$141 \quad FR_{total}(t) = \left(\frac{d_d(t) + d_{ud}(t)}{c_d(t) + c_{ud}(t)} \right) \quad (4)$$

142 $FR_{reported}$ is commonly known as the case fatality rate, and FR_{total} is the infection fatality
143 rate.

144 *Estimating the proportion of detected deaths using a predictive model*

145 We predicted the detection ratio among death cases using daily values of five indicators related
146 to testing, tracing, and hospital capacities as candidate predictors. These indicators are: the
147 *proportion of cases without contact tracing delay, ratio of the number of tests conducted to*
148 *reported cases, testing delay, reporting delay and death delay* (for definitions, see **Error!**
149 **Reference source not found.**). We calculated the delay periods in testing, reporting and death
150 by subtracting adjusting for the date of symptom onset from the dates of these three events.
151 Testing (the first test) earlier or on the same day as symptom onset implied that cases were

152 contact-traced without delay. If cases were tested after symptom onset, they were either
153 contact-traced with delay or were not contact-traced. The proportion of death cases that were
154 contact-traced without delay was calculated.

155 To investigate the factors that influence the proportion of detected deaths, we developed a
156 logistic regression model. We assumed that the number of deaths that were previously detected
157 on day t follows a binomial distribution, i.e. $d_d(t) \sim \text{binomial}(d(t), m(t))$, where $m(t) =$
158 $\frac{d_d(t)}{d_d(t) + a_{ud}(t)}$ is the expected proportion of detected deaths on day t .

159 The full predictive model is:

$$160 \quad \log\left(\frac{m(t)}{1 - m(t)}\right) = \alpha + \beta_1 R_{tc} + \beta_2 P_{ntd} + \beta_3 C_d + \beta_4 T_d + \beta_5 D_d \quad (5)$$

161 where R_{tc} is the daily ratio of tests conducted to reported cases; P_{ntd} represents the daily
162 proportion of cases (among detected deaths) without contact tracing delay. C_d , T_d and D_d are
163 daily reporting, testing and death delays, respectively. α is the intercept and β_i is the regression
164 coefficient of each covariate. The proportion of undetected COVID-19 cases can be calculated
165 using equations (1) and (5) after $m(t)$ is estimated:

$$166 \quad \frac{c_{ud}(t)}{c_{ud}(t) + c_d(t)} = 1 / \left(1 + \frac{m(t)}{1 - m(t)} \times \frac{FR_{ud}}{FR_d(t)} \right) \quad (6)$$

167 where $\frac{m(t)}{1 - m(t)} = \frac{d_d(t)}{a_{ud}(t)}$ is the odds of being detected.

168 **Model selection**

169 To obtain the best model, the variables in equation 5 were added to the model iteratively. First,
170 model fit was measured for each of the variables separately using the Akaike information
171 criterion (AIC) ¹³. The model containing the lowest AIC value was selected as the best model
172 candidate in this batch. Next, we added one additional variable to the candidate model from
173 the remaining four variables in the next batch. Among the two-variable models, the model with
174 the lowest AIC value was selected as the best model candidate again. We obtained the best
175 model candidates among three-variable, four-variable and full models. The final best model
176 was obtained by comparing the best model candidates in different batches with the lowest AIC.

177 **Model validation**

178 To evaluate whether the predictive model achieved its intended purpose (i.e., to improve the
179 accuracy of epidemiological parameter estimation), we explored the relationship between R_t

180 estimated from the total cases predicted by the best model and daily mobility data. Cases
181 were back-projected to infection time. The result was compared with R_t estimated using total
182 cases that were empirically derived or using reported cases. R_t estimated from four scenarios
183 of infections were compared:

184 **Scenario 1 (S1): Total cases (at infection time) estimated using an empirical detection**
185 **ratio** – These cases include both the reported and undetected cases at their infection time. The
186 number of undetected cases was estimated empirically assuming reporting delay was the same
187 for detected and undetected cases.

188 **Scenario 2 (S2): Total cases (at infection time) estimated from a model-predicted**
189 **detection ratio** – These cases include both the reported and undetected cases at their infection
190 time. The number of undetected cases was estimated from the model assuming reporting delay
191 was the same for detected and undetected cases.

192 **Scenario 3 (S3): Reported cases (at infection time)** – Cases that were detected before death
193 and late-detected after death at their infection time.

194 **Scenario 4 (S4): Reported cases (at reporting time)** – Cases that were detected before death
195 and late-detected after death at their reporting time. Late-detected cases were back-projected
196 at the adjusted reporting time.

197 *Estimating the effective reproduction number*

198 The effective reproduction number R_t was estimated from the daily new cases of infection
199 using the statistical package *EpiEstim*¹⁴. To estimate the daily number of new cases, we
200 assumed that both the incubation time and reporting delay followed gamma distribution^{15,16}.
201 The mean incubation time for the circulated strain in Taiwan was 3.53 days¹⁷, and we estimated
202 the mean reporting delay as 4.45 days. Assuming the standard deviations were equal for both
203 the distributions (estimated as 3.93 days for the reporting delay), the distribution of time
204 between infection and reporting was gamma distribution with a mean of 7.98 days and a
205 standard deviation of 5.28 days. The mean of the distribution was estimated as the sum of mean
206 incubation time and confirmation delay. In contrast, the standard deviation was obtained from
207 weighted means and pooled standard deviation for the period between infection and reporting
208 using the following formula:

$$209 \quad sd_{gamma} = sd_{pooled} \sqrt{\left(\frac{m_1 + m_2}{m_w}\right)} \quad (7)$$

210 where, m_1 and m_2 are mean incubation time and confirmation delay and m_w refers weighted
211 mean of these two. sd_{pooled} represents the pooled standard deviation for the period between
212 infection and reporting.

213 We then estimated total cases at infection time using the empirical detection ratio (S1) and the
214 model-predicted detection ratio (S2), and reported cases at infection time (S3) using a back-
215 projection method ¹².

216 We set initial conditions for estimating R_t . Before May 11, we assumed that there were 15
217 cases each day between May 6 and 10, which was the average number of reported cases at
218 infection time during this 5-day period.

219 **Results**

220 Time-varying FR among true total cases (equation 4) was first quantified after taking into
221 account undetected cases and was compared with that of reported cases. The number of total
222 cases was also predicted using polymerase chain reaction (PCR) testing data (equations 5 and
223 6). To assess the impact of including undetected cases, we investigated the relationship between
224 R_t generated using total cases and mobility data and then determined whether the relationship
225 improved, compared with R_t from reported cases.

226 After the number of undetected cases was considered, the estimated FR was lower than using
227 reported cases but was still high during the initial period of the outbreak. The mean FR of total
228 cases was estimated to be 4.7%, which was lower than the mean FR of 5.3% for reported cases
229 ([Figure 1B](#)). The FR increased rapidly from 4.7% and peaked at 6.5% on May 19, but then
230 continued decreasing, reaching 2.8% on June 6. Since then, the rate was generally maintained.

231 From May 24 to June 3, the 5-day moving average numbers of reported cases reached a plateau
232 and then declined thereafter ([Figure 3A](#)). The estimated true daily case number at the peak of
233 the outbreak on May 22 was 897, which was 24.3% higher than the reported number. The
234 difference became less than 4% on June 9 and afterward.

235 Until June 20, a total of 105 late-detected cases were reported, indicating many undetected
236 deaths. Similarly, daily detected deaths also reached a plateau around May 24 ([Figure 3B](#)).
237 However, the number of late-detected cases (at adjusted reporting time), reached a peak (7
238 persons per day) on May 21 and started to decline immediately, approaching zero after June 8.
239 This indicated the improvement of the detected ratio among deaths. The detection ratio among
240 deaths, which was about 50% initially, exceeded 95% after the end of May ([Figure S1B](#)). This
241 ratio was very different from the observed ratio (a V-shaped pattern) without back-projection
242 ([Figure S1A](#)).

243 ***Predicting detection ratio using testing data***

244 We next investigated whether the improvement in the proportion of detected cases was related
245 to the improved capacity of testing and tracing. The indicators of the capacity were explained
246 by the schematic of individual infection and testing statuses of each case among deaths (for
247 definitions, please refer to [Figure 2](#) and its legend). Depending on the time of testing, the case
248 can be categorized as a detected death (contact-traced without delay or tested after symptom
249 onset but before death) or an undetected death (tested after death). More efficient contact

250 tracing allowed more cases to be traced and tested before symptom onset and was indicated by
251 the *proportion of cases without contact tracing delay*. This proportion fluctuated between 25%
252 and 75% throughout the study period, with an increasing trend from late May (below 50%) to
253 late June (above 60%) ([Figure 4A](#)). The *testing delay* gradually increased, from approximately
254 two days to up to 4–6 days, until June 14, a few weeks after the outbreak started to decline
255 ([Figure 4B](#)). The *reporting delay* from the day of symptom onset ranged mostly between 2.5
256 and 7.5 days ([Figure 4E](#)), whereas the *death delay* continued increasing from 5 days to more
257 than 18 days ([Figure 4C](#)). The *ratio of the number of tests conducted to reported cases*
258 increased from less than 50 to more than 200 ([Figure 4D](#)), demonstrating the improvement in
259 testing capacity throughout the outbreak.

260 We compared models starting from the most basic to more complex ones by their AIC values
261 to identify the best-fitting model. The model with the predictor, i.e., the proportion of cases
262 without contact tracing delay and the ratio of tests conducted to reported cases, was selected as
263 the best model (Model 2 in [Table 1](#)).

264 The model successfully captured the trend in the proportion of detected deaths ([Figure 4F](#)). 20
265 out of 34 daily values were successfully predicted within the confidence interval. Among the
266 values outside the interval, most of the them were in the near distance; only two dots have
267 errors larger than two times the intervals.

268 The results suggest that a higher detection ratio among deaths was driven by more cases who
269 were contact-traced without delay and a higher number of tests conducted relative to the
270 number of cases ([Table 2](#)).

271 *Comparing effective reproduction number and mobility index*

272 Comparisons were made between R_t estimated using i) total cases that were estimated using
273 the empirical detection ratio; ii) total cases that were estimated from the model-predicted
274 detection ratio using testing data; and iii) reported cases only (see [Figure 5A, B](#), [Figure S2](#) and
275 Methods). When the total case number was used, R_t was higher during the earlier dates. The
276 number reached a maximum value of 6.4 on May 11, compared to 6.0 estimated using the
277 reported case number. We further evaluated the relationship between R_t and mobility data
278 during the period when R_t reduced from the maximum value to 1 (May 11 to May 24) ([Table](#)
279 [S1](#)). We found that when the total case number was used (either estimated using the empirical
280 detection ratio or predicted using the testing data), a lower AIC was produced, indicating a
281 better fit to the mobility data.

282 In summary, efficiencies of testing and contact tracing changed during the outbreak and were
283 useful in predicting the proportion of undetected cases. After adding the undetected cases, a
284 better estimate of R_t was made and a reduction in the FR was observed.

285 Discussion

286 Understanding whether a high FR observed in the recent largest COVID-19 outbreak in Taiwan
287 was attributed to a higher number of undetected cases or insufficient health care capacity is
288 important to guide interventions to reduce COVID-19 mortality in the future. An important
289 observation is that even though the proportion of undetected cases was included, the average
290 FR was only adjusted to 4.7% from 5.3%, which is still higher than the global average for the
291 same time (i.e., 2.1% in May and June 2021⁵). However, the daily FR reduced to 2.8% on June
292 6 and remained at this low level, similar to that in the United States (i.e., 2.8% in May and June
293 2021¹⁸). The reduction from the initially high FR can be explained by the improvement in
294 hospital capacity or treatment to accommodate the sudden rise in cases. This is supported by
295 the observation that the duration between symptom onset and death among detected deaths
296 continued increasing from approximately five days to more than two weeks in June.

297 The number of hidden (undetected) COVID-19 cases often affects the estimation of
298 transmissibility of the virus and the effectiveness of non-pharmaceutical interventions (NPIs)
299 implemented. Even though the effects of contact tracing and testing on transmissibility have
300 been studied^{19,20}, how many hidden cases do they cause is unclear. We demonstrated that the
301 time-varying detection ratios can be predicted using data on testing and contact tracing. As a
302 result, a more accurate R_t can be obtained, which is likely to be explained by mobility data
303 better. The guidance for implementing NPIs based on changes in mobility can be provided⁸.

304 We found that the ratio of the number of tests conducted to reported cases, and the proportion
305 of cases that are contact traced without delay can be used to “nowcast” the proportion of
306 undetected cases. Because the number of tested samples can quickly reach the capacity limit
307 when the case number is growing, many samples remain untested. Hence, each day, the number
308 of confirmed cases depends largely on how many tests can be performed. A day delay in testing
309 and confirming a case, leads to a day delay in tracing the close contacts of the case. Further
310 more, a higher contact tracing coverage together with a shorter delay of being traced enables
311 more cases to be identified earlier^{19,20}. These suggest increasing testing and tracing capacity to
312 identify those infections earlier can reduce hidden cases more.

313 Modelling has been used to estimate the proportion of undetected COVID-19 cases using the
314 observed case number during a specific period (e.g., before or after an intervention) of an
315 outbreak^{21,22}. More recently, an approach through estimating under-ascertainment by directly
316 comparing model-predicted death with excess deaths recorded was used²³. We checked the

317 number of deaths related to flu and pneumonia illness ⁹ and found no unusual excess deaths
318 other than the reported COVID-19 deaths during this period. The proportion of undetected
319 cases can also be calculated after incorporating seroprevalence data with false negative rates
320 of tests into models ²⁴. Overall, none of these methods estimate the constantly changing
321 proportion of undetected cases.

322 Several criteria enabled us to make successful prediction using testing data. First, the number
323 of deaths should be high. If this number is low, the uncertainty of estimating the number of
324 undetected cases becomes high. Second, most of the deaths have to be tested eventually.
325 Taiwan government has a strong directive to test all sudden death cases; for example, on June
326 18, it was announced that PCR tests would be performed for all sudden and unexplained deaths
327 ²⁵. This may not likely be the case in countries with a large number of excess deaths associated
328 with COVID-19.

329 In summary, predicting the number of undetected cases as early as possible using testing data
330 can help obtain an R_t with a better relationship with mobility data, thus enabling policymakers
331 to make timely public health decisions using mobility information to contain the outbreak.

332 **Acknowledgement**

333 The authors are indebted to City University of Hong Kong for providing excellent research
334 facilities. The authors also acknowledge support from grants funded by Health and Medical
335 Research Fund [COVID190215] and City University of Hong Kong [7200573 and 9610416].

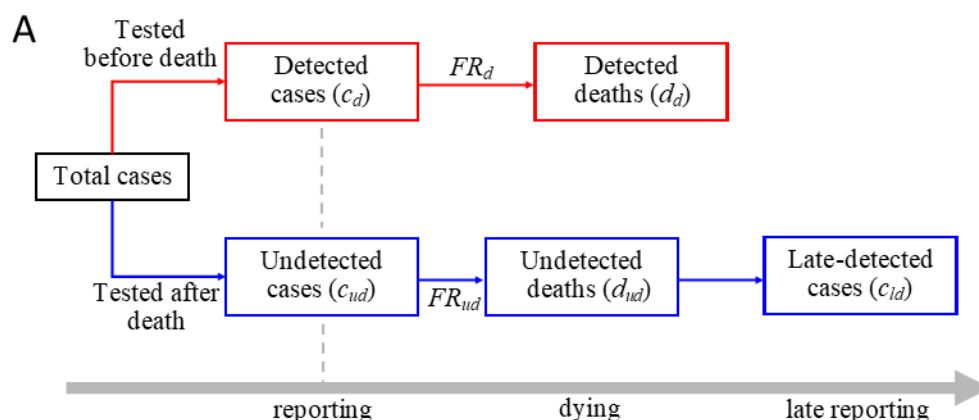
336 **References**

- 337 1. Grassly, N. C., Pons-Salort, M., Parker, E. P. K., White, P. J. & Ferguson, N. M.
338 Comparison of molecular testing strategies for COVID-19 control: a mathematical
339 modelling study. *Lancet Infect. Dis.* **20**, (2020).
- 340 2. Contreras, S. *et al.* The challenges of containing SARS-CoV-2 via test-trace-and-isolate.
341 *Nat. Commun.* **12**, 1–13 (2021).
- 342 3. Tan, Y. COVID-19: What went wrong in Singapore and Taiwan? - BBC News. *BBC*
343 *News* <https://www.bbc.com/news/world-asia-57153195> (2021).
- 344 4. Taiwan National Infectious Disease Statistics System. Severe Pneumonia with Novel
345 Pathogens (COVID-19). <https://nidss.cdc.gov.tw/en/nndss/disease?id=19CoV> (2021).
- 346 5. Our World in Data. Coronavirus (COVID-19) Deaths - Statistics and Research.
347 <https://ourworldindata.org/covid-deaths> (2021).
- 348 6. Taiwan Centers for Disease Control. CECC raises epidemic warning to Level 2 and
349 implements related restrictions and measures, effective from May 11 to June 8, in
350 response to increased risk of community transmission.
351 [https://www.cdc.gov.tw/En/Bulletin/Detail/0jMlImCVWTuhO9mfQCd-](https://www.cdc.gov.tw/En/Bulletin/Detail/0jMlImCVWTuhO9mfQCd-4g?typeid=158)
352 [4g?typeid=158](https://www.cdc.gov.tw/En/Bulletin/Detail/0jMlImCVWTuhO9mfQCd-4g?typeid=158) (2021).
- 353 7. Taiwan Centers for Disease Control. CECC raises epidemic warning to Level 3
354 nationwide from May 19 to May 28; strengthened measures and restrictions introduced
355 across Taiwan to reduce community transmission.
356 https://www.cdc.gov.tw/En/Bulletin/Detail/VN_6yeoBTKhRkKoSy2d0hJQ?typeid=158
357 (2021).
- 358 8. Nouvellet, P. *et al.* Reduction in mobility and COVID-19 transmission. *Nat. Commun.*
359 **12**, 1–9 (2021).
- 360 9. Taiwan Centers for Disease Control. COVID-19 (SARS-CoV-2 Infection).
361 <https://www.cdc.gov.tw/En>.
- 362 10. Government Information Open Platform. Taiwan's COVID-19 coronavirus test daily
363 delivery number. <https://data.gov.tw/dataset/120451> (2021).
- 364 11. Taiwan daily confirmed local case data.

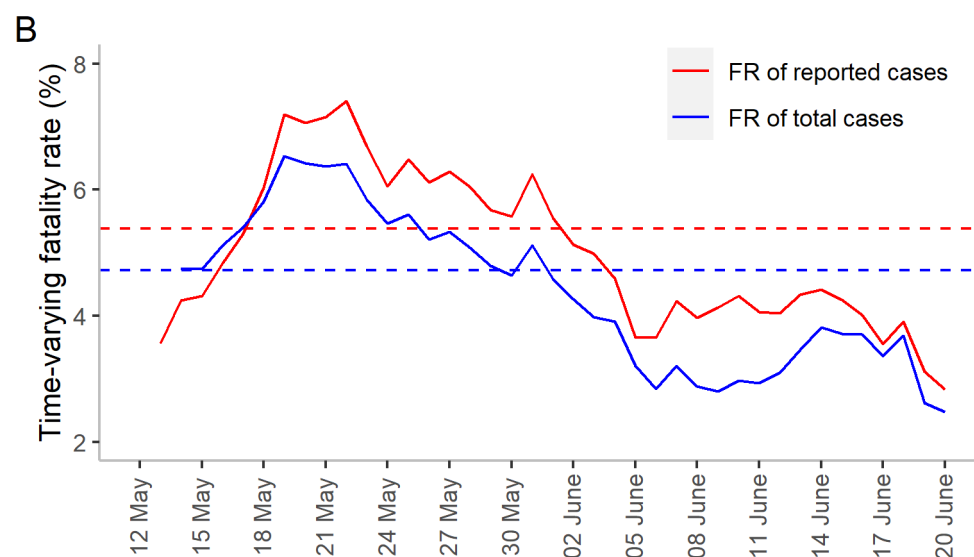
- 365 [https://docs.google.com/spreadsheets/d/12tQKCRuaiBZfc9yDd6tmlOds62ke_4AcK](https://docs.google.com/spreadsheets/d/12tQKCRuaiBZfc9yDd6tmlOds62ke_4AcKmNJ6q4gdU/)
366 [mNJ6q4gdU/](https://docs.google.com/spreadsheets/d/12tQKCRuaiBZfc9yDd6tmlOds62ke_4AcKmNJ6q4gdU/) (2021).
- 367 12. Becker, N. G., Watson, L. F. & Carlin, J. B. A method of non-parametric back-projection
368 and its application to aids data. *Stat. Med.* **10**, 1527–1542 (1991).
- 369 13. Bozdogan, H. Model selection and Akaike’s Information Criterion (AIC): The general
370 theory and its analytical extensions. *Psychometrika* **52**, 345–370 (1987).
- 371 14. Cori, A., Ferguson, N. M., Fraser, C. & Cauchemez, S. A New Framework and Software
372 to Estimate Time-Varying Reproduction Numbers During Epidemics. *Am. J. Epidemiol.*
373 **178**, 1505–1512 (2013).
- 374 15. Adam, D. C. *et al.* Clustering and superspreading potential of SARS-CoV-2 infections
375 in Hong Kong. *Nat. Med.* **26**, 1714–1719 (2020).
- 376 16. Qin, J. *et al.* Estimation of incubation period distribution of COVID-19 using disease
377 onset forward time: A novel cross-sectional and forward follow-up study. *Sci. Adv.* **6**,
378 eabc1202 (2020).
- 379 17. Homma, Y. *et al.* The incubation period of the SARS-CoV-2 B.1.1.7 variant is shorter
380 than that of other strains. *J. Infect.* **83**, e15–e17 (2021).
- 381 18. Worldometer. COVID-19 coronavirus pandemic.
382 <https://www.worldometers.info/coronavirus/> (2021).
- 383 19. Kretzschmar, M. E. *et al.* Impact of delays on effectiveness of contact tracing strategies
384 for COVID-19: a modelling study. *Lancet Public Heal.* **5**, e452–e459 (2020).
- 385 20. Kucharski, A. J. *et al.* Effectiveness of isolation, testing, contact tracing, and physical
386 distancing on reducing transmission of SARS-CoV-2 in different settings: a
387 mathematical modelling study. *Lancet Infect. Dis.* **20**, 1151–1160 (2020).
- 388 21. Liang, J., Yuan, H.-Y., Wu, L. & Pfeiffer, D. U. Estimating effects of intervention
389 measures on COVID-19 outbreak in Wuhan taking account of improving diagnostic
390 capabilities using a modelling approach. *BMC Infect. Dis.* **21**, 1–10 (2021).
- 391 22. Li, R. *et al.* Substantial undocumented infection facilitates the rapid dissemination of
392 novel coronavirus (SARS-CoV-2). *Science* **368**, 489–493 (2020).
- 393 23. Watson, O. J. *et al.* Leveraging community mortality indicators to infer COVID-19

- 394 mortality and transmission dynamics in Damascus, Syria. *Nat. Commun.* **12**, 1–10
395 (2021).
- 396 24. Bhattacharyya, R. *et al.* Incorporating false negative tests in epidemiological models for
397 SARS-CoV-2 transmission and reconciling with seroprevalence estimates. *Sci. Rep.* **11**,
398 1–14 (2021).
- 399 25. Taiwan Centers for Disease Control. Report on the Press Conference after the National
400 Epidemic Prevention Conference on June 18-Department of Disease Control, Ministry
401 of Health and Welfare.
402 <https://www.cdc.gov.tw/Bulletin/Detail/j5bFJQGngMHxaaQIK-j12w?typeid=9> (2021).
- 403 26. google. COVID-19 Community Mobility Reports.
404 <https://www.google.com/covid19/mobility/?hl=en-GB> (2021).
- 405

406 **Figures and tables**

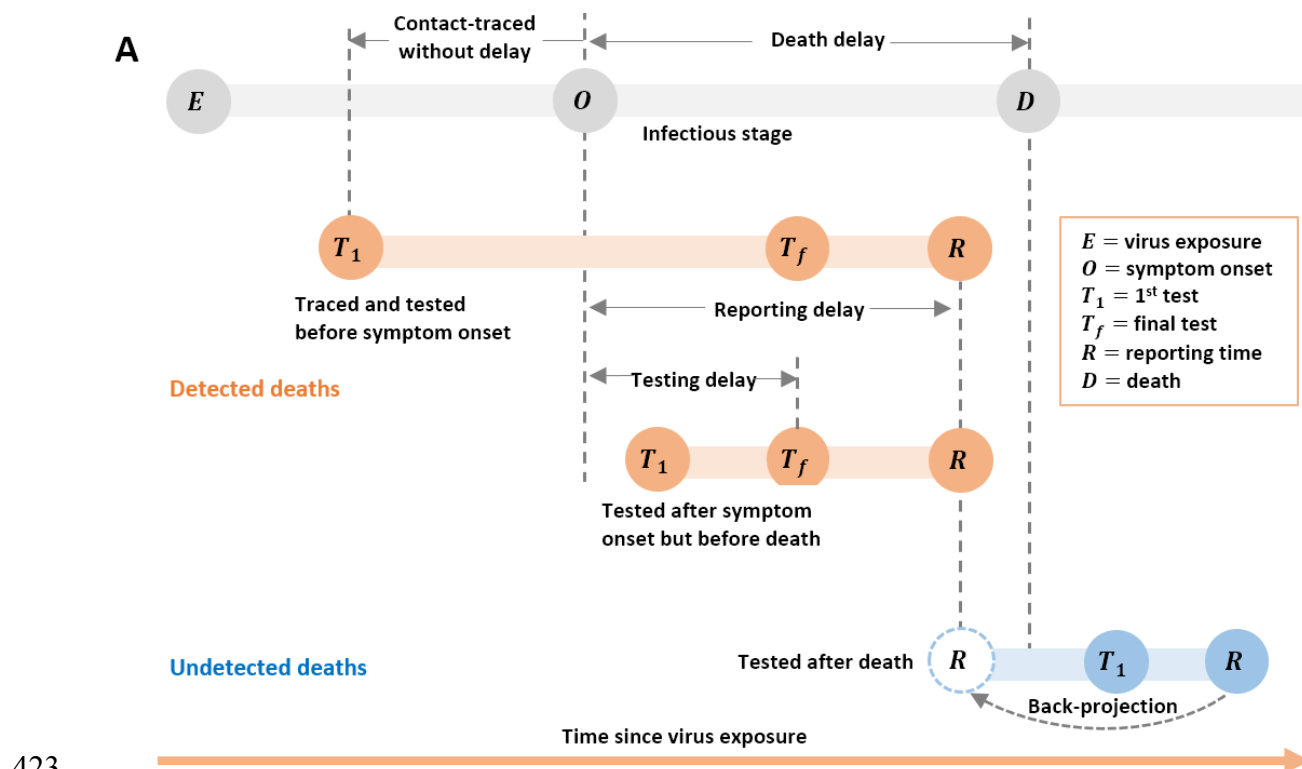


407

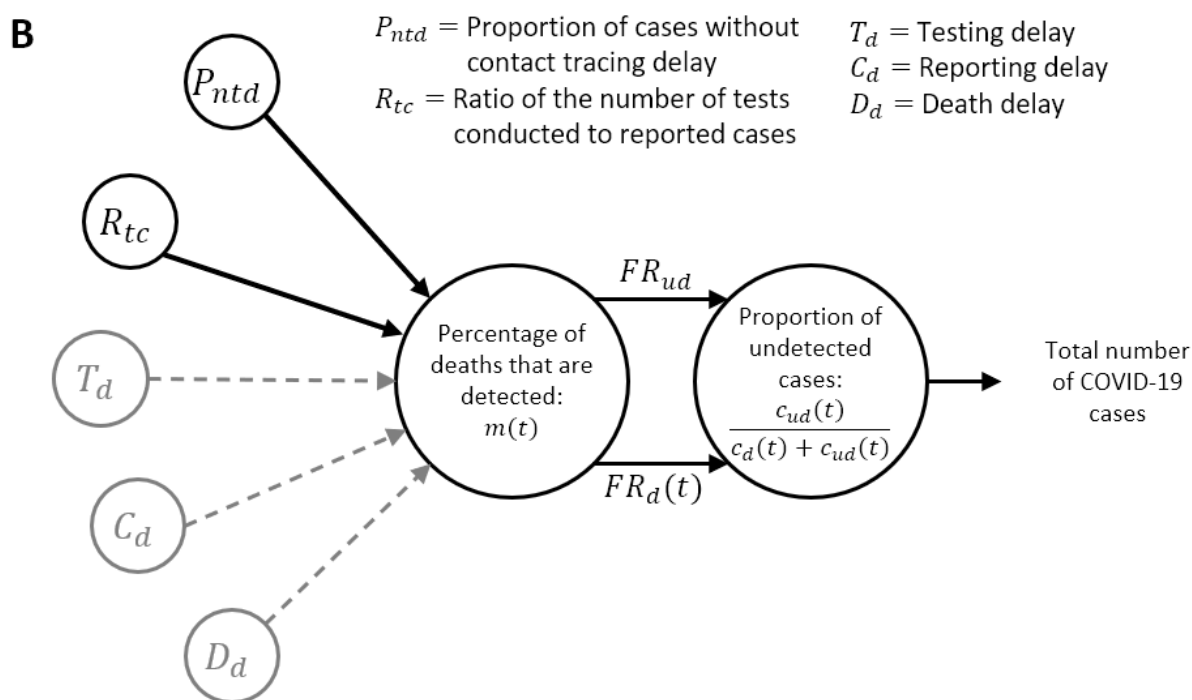


408

409 Figure 1. Types of cases and the fatality rate (FR). (A) Schema of different types of cases and
 410 deaths in relation to their testing and death time. At the time of reporting detected cases, the
 411 number of undetected cases is estimated using Eq. (2) (see Methods). FR_d is the FR among
 412 detected cases, and FR_{ud} is the FR among undetected cases. Reported cases include both
 413 detected and late-detected cases (after undetected deaths are tested and confirmed), while total
 414 cases include both detected and undetected cases. (B) Time-varying FRs among reported and
 415 total cases. The solid red line represents the proportion of reported deaths (i.e., detected and
 416 undetected deaths) among the total reported cases. The solid blue line represents the proportion
 417 of reported deaths among the total cases. The dashed red line represents the average FR among
 418 the reported cases (5.3%), whereas the blue dashed line shows the average FR among the total
 419 cases (4.7%). Note that the FR of the total cases was higher than that of the reported cases in
 420 the first few days because FR_{ud} was assumed to be same as the mean FR_d between May 11
 421 and May 26. Data points during the earliest dates when the number of detected or undetected
 422 cases was zero are not shown.



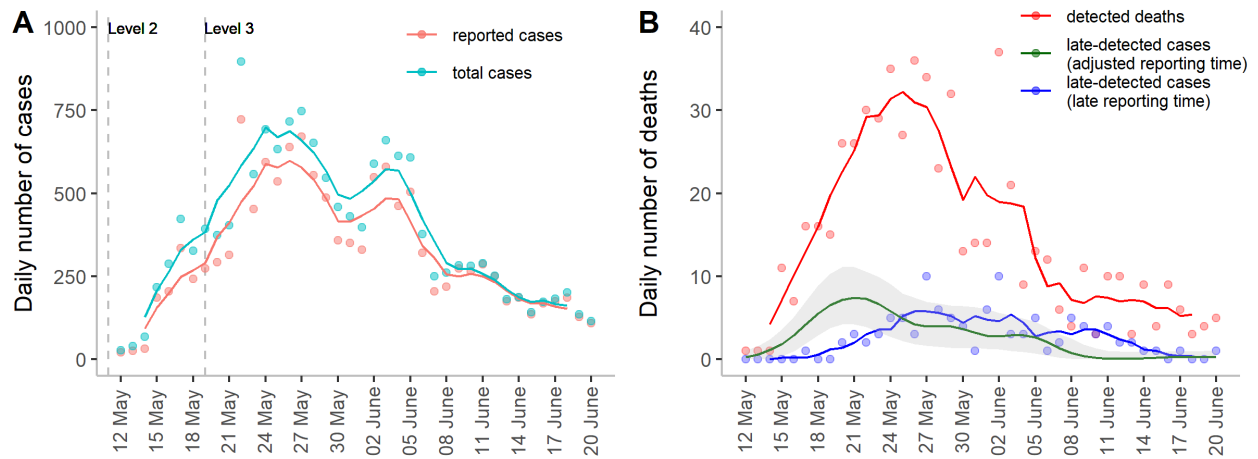
423



424

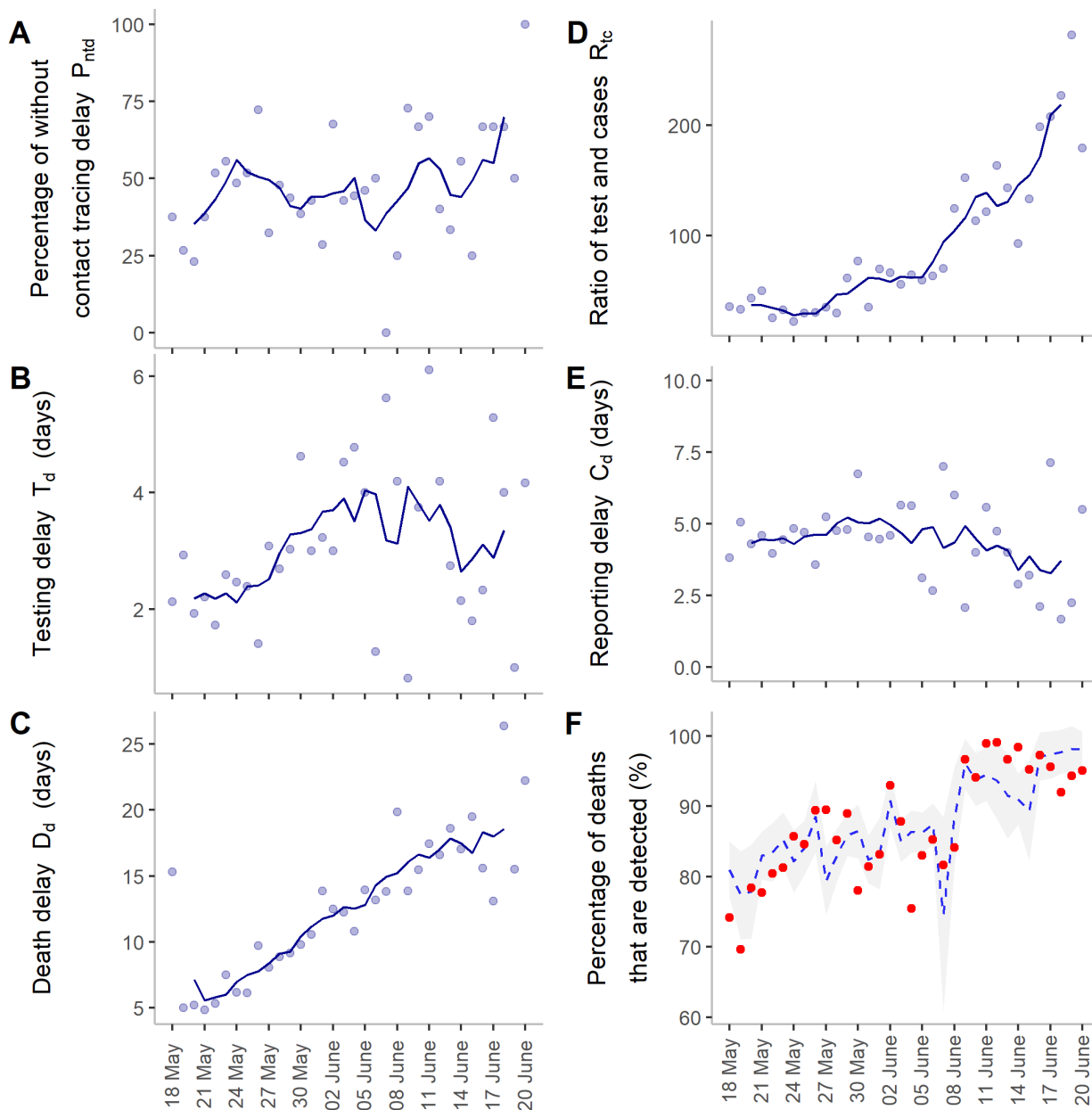
425 Figure 2. (A) Statuses of infection and testing of individual deaths. The gray bar represents the
 426 infection statuses of an infected case who later died after the start of infection. Orange and blue
 427 bars represent the flow of testing from the first test until the infected case is reported. The
 428 infected case was categorized as *Detected* if the first testing was performed before death. A
 429 case that was tested on the same date of or after death was categorized as *Undetected*. Among
 430 detected cases, we assumed that a case was contact traced without delay if the first test T_1 was
 431 performed before symptom onset O ; otherwise, contact traced with delay or not contact traced
 432 if the T_1 was performed after symptom onset. Testing delay refers to the time between symptom
 433 onset and the last test T_f . Similarly, the reporting delay and death delay are defined as the time

434 difference between symptom onset and reporting, R , and death, D , respectively. The reporting
435 time among an undetected death was adjusted to an earlier time to have the same reporting
436 delay as detected deaths. The definitions for each status, E , O , T_1 , T_f , R and D , are listed in the
437 text box. **(B) Estimation of total number of COVID-19 cases (sum of detected and**
438 **undetected) using a regression model.** With the best-fitting model (see [Table 2](#)), we estimated
439 the percentage of deaths that are detected, $m(t)$. Undetected proportion of cases was estimated
440 based on the relationship between $m(t)$ and fatality rates (see equation 6). Gray dashed lines
441 represent the predictors that were not included in the best-fitting model while estimating $m(t)$.

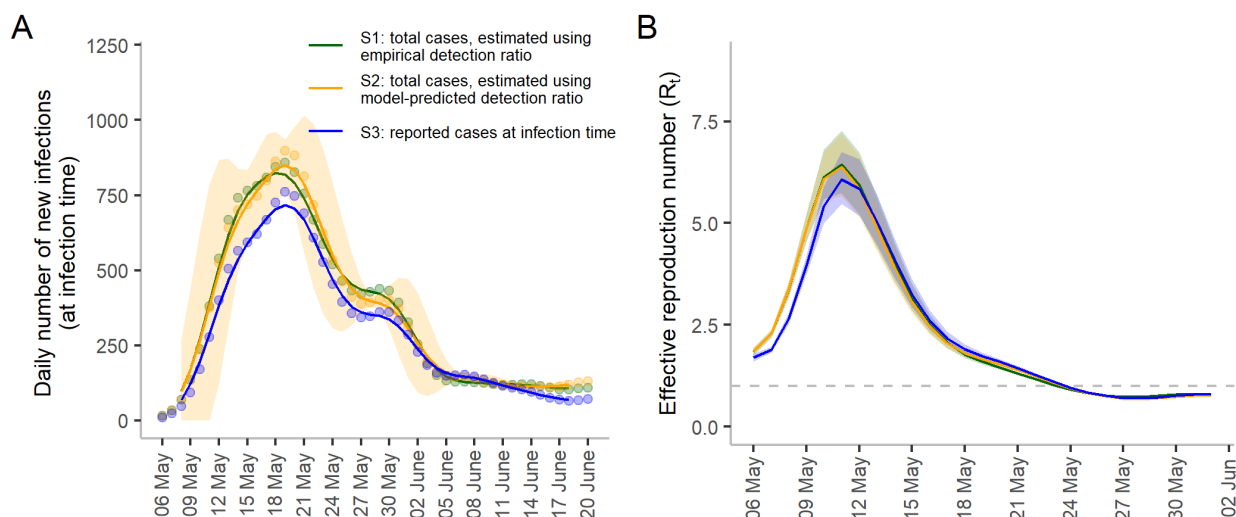


442

443 Figure 3. Daily numbers of reported, total cases and deaths. Data are plotted on their reporting
444 date. **(A)** Daily number of cases that are reported. Daily number of total cases, including both
445 the detected and undetected cases at their reporting date (green). The reporting delay of
446 undetected cases is adjusted to be the same as that of the reported cases. The dashed vertical
447 lines represent the implementation of level 2 and level 3 restrictions in May and June. Level 2
448 restrictions were started on May 11 and lasted until June 8, whereas level 3 restrictions were
449 started on May 19 and lasted until May 28. **(B)** Daily number of deaths, plotted separately for
450 detected deaths at their reporting time following case confirmation (red),) late-detected cases
451 at adjusted reporting time (dark green) and late-detected cases at their late reporting time (blue).
452 Dots represent daily numbers. Solid lines represent moving averages using a 5-day sliding
453 window, centered at day 3 (except dark green line in (B)).



454
 455 Figure 4. Candidate predictors that influence detected deaths. Dots in each plot represent
 456 observed values, whereas solid lines show moving averages using a 5-day sliding window,
 457 centered at day 3. **(A)** Percentage of cases without contact tracing delay was defined as the
 458 proportion of cases that were tested (the first test) earlier or on the same day as symptom onset.
 459 **(B)** Testing delay is the time delay between symptom onset and the final test. It was estimated
 460 by subtracting these two time points. **(C)** Death delay was defined as the difference between
 461 the time of death and symptom onset. **(D)** Ratio of tests to cases was calculated as the daily
 462 number of tests divided by the daily number of reported cases. **(E)** Reporting delay refers to
 463 the time delay between symptom onset and reporting. **(F)** Percentage of deaths that are detected
 464 using adjusted reported data and model prediction. Red circles represent the adjusted reported
 465 data. The blue dashed line represents the prediction results using the best fitting model. The
 466 gray shaded area represents forecasted values of the proportion of detection.



467
468 Figure 5. The daily number of new infections and instantaneous reproduction numbers. (A)
469 The daily number of new infections was back-projected from the daily number of cases
470 obtained from the detected and empirically estimated undetected cases (green dots; referred to
471 as S1). The daily number of new infections obtained from the detected and model-predicted
472 undetected cases were plotted (dark yellow dots; referred to as S2). The daily number of
473 reported cases at their back-projected infection time (blue dots; referred to as S3). The daily
474 numbers of new infections were back-projected from the original reported cases to virus
475 exposure time. The lines represent moving averages using a 5-day sliding window, centered at
476 day 3. The shaded area represents the 95% confidence interval for total cases estimated using
477 the model-predicted detection ratio. Daily number of new detected (reported) cases at their
478 reporting time (red dots; referred to as S4) is presented in Figure S2. (B) Effective reproduction
479 number estimated from (A). Lines represent the estimated values and shaded regions represent
480 the 95% confidence intervals. The dashed line depicts the cutoff value when $R_t = 1$. The full
481 view of the effective reproduction number (R_t) for the entire period between May 6 and June
482 20 is given in Figure S4. Color codes represent the same definition as in (A). The shaded area
483 represents 95% confidence intervals.

484

485 Table 1. Candidate models used to choose the best model. α and β s are model coefficients,
486 whereas the proportion of contact tracing delay (P_{ntd}), the ratio of the number of tests
487 conducted and reported cases (R_{tc}), the delay in testing (T_d), the delay in reporting (C_d), and
488 the delay in deaths (D_d) are predictors. AIC represents the Akaike information criterion.

Models	Description	AIC
1	$\alpha + \beta_1 R_{tc}$	95.9
2	$\alpha + \beta_1 R_{tc} + \beta_2 P_{ntd}$	91.0
3	$\alpha + \beta_1 R_{tc} + \beta_2 P_{ntd} + \beta_3 C_d$	93.0
4	$\alpha + \beta_1 R_{tc} + \beta_2 P_{ntd} + \beta_3 C_d + \beta_4 T_d$	95.0
5	$\alpha + \beta_1 R_{tc} + \beta_2 P_{ntd} + \beta_3 C_d + \beta_4 T_d + \beta_5 D_d$	96.9

489

490

491

492 Table 2. Parameter estimates of the best-fitting model (Model 2)

Covariates	Estimates	95% Confidence intervals	p-value
Ratio of number of tests conducted to reported cases (R_{tc})	0.009	0.002-0.018	0.0180
Proportion of cases without tracing delay (P_{ntd})	1.834	0.316-3.375	0.0185

493

494

495 **Supplementary Materials**

496 ***Establishing the relationship between mobility and effective reproduction number***

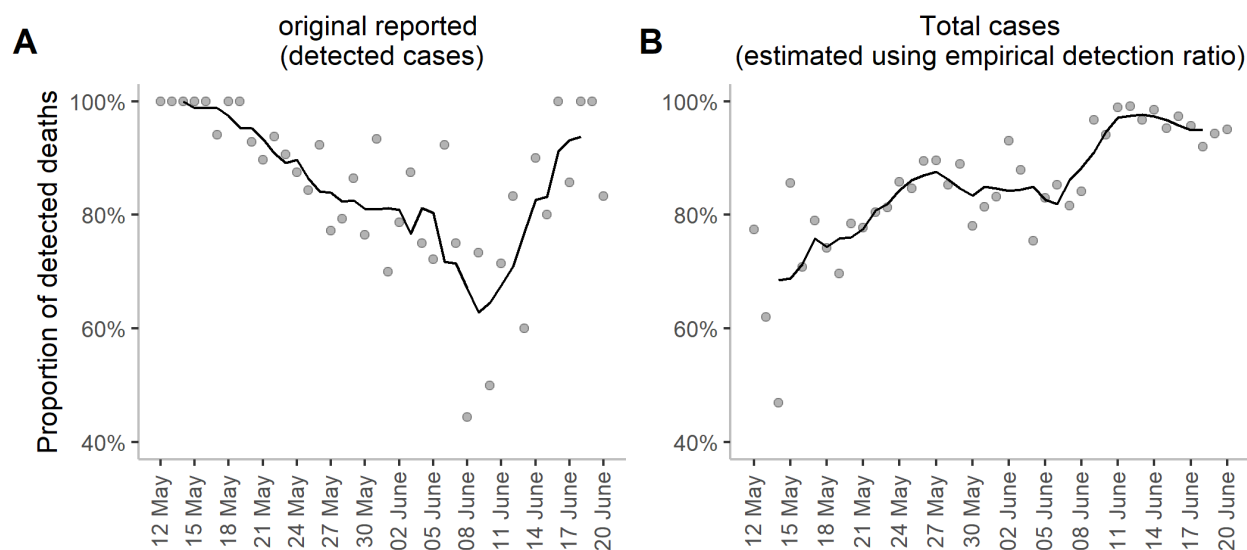
497 Daily mobility data were obtained from Google mobility report ²⁶ and were normalized after
498 setting the mobility index on May 11 (first day of the start of the outbreak) as 1 and the value
499 -100 as 0. The normalized mobility index ranged between 0 and 1, where higher values
500 represent greater mobility. To compare and validate the estimated R_t , we used a generalized
501 linear model for Gaussian distribution with identity link function. Mobility index was adjusted
502 in the model using the following formula adopted from a recent study ⁸:

503
$$\log(R_t) = \log(R_0) + \beta(1 - M_b(t)). \quad (8)$$

504 where R_0 is the initial reproduction number obtained from R_t at the start of the outbreak (May
505 11, 2021), which gave the maximum number of R_t ; $M_b(t)$ represents the daily normalized
506 mobility index; and β is the regression coefficient.

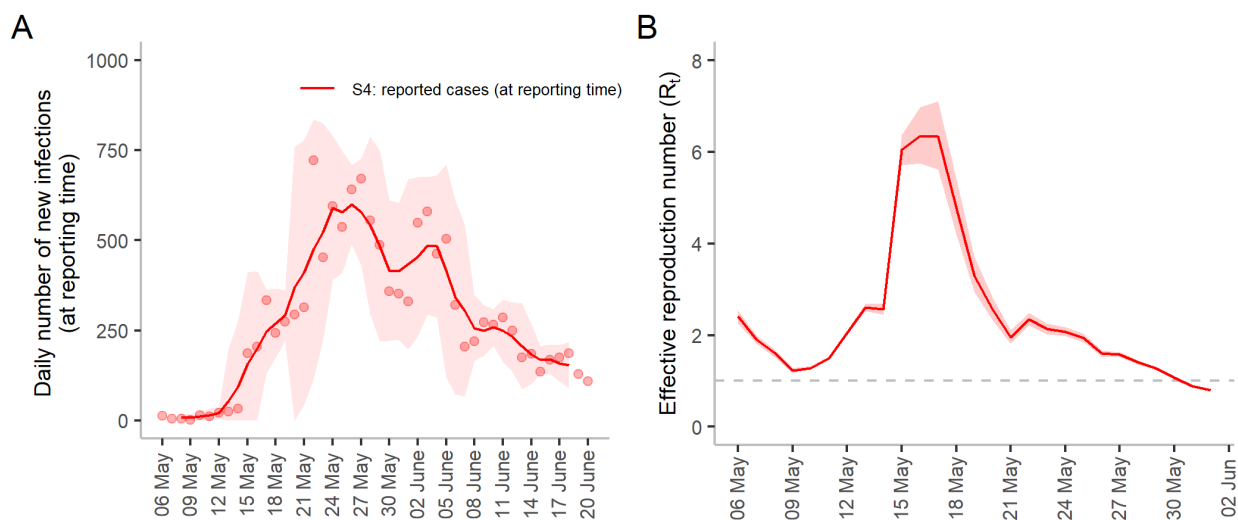
507 **Supplementary figures**

508



509
510

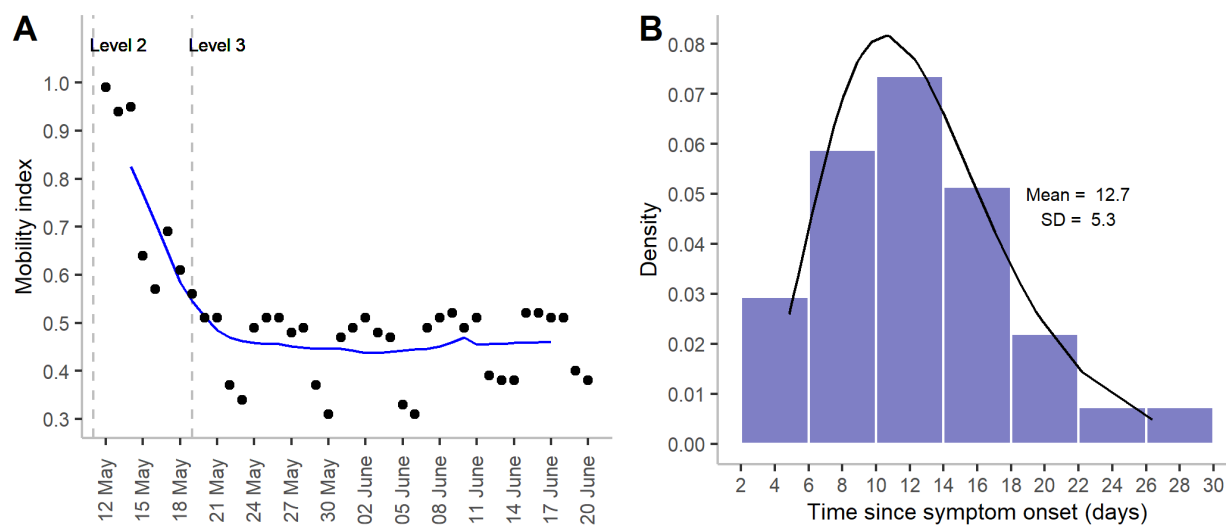
511 Figure S1. **(A)** Proportion of detected deaths among total reported deaths. **(B)** Proportion of
512 detected deaths among total deaths estimated using the empirical detection ratio. In each plot,
513 dots represent daily numbers that are observed or estimated. Solid lines represent moving
514 average using a 5-day sliding window, centered at day 3.



515
516

517 Figure S2. **(A)** Daily number of new infections at their reporting time. Daily values are
518 indicated by red dots (referred to as S4 in Methods). The line represents moving averages using
519 a 5-day sliding window, centered at day 3. **(B)** Effective reproduction number estimated from
520 (A). The solid red line represents estimated values. The shaded area represents 95% confidence
521 intervals. The dashed line depicts the cutoff value when $R_t = 1$. The value R_t during the entire
522 period (between May 6 and June 20) is given in the Supplementary Figure S4D.

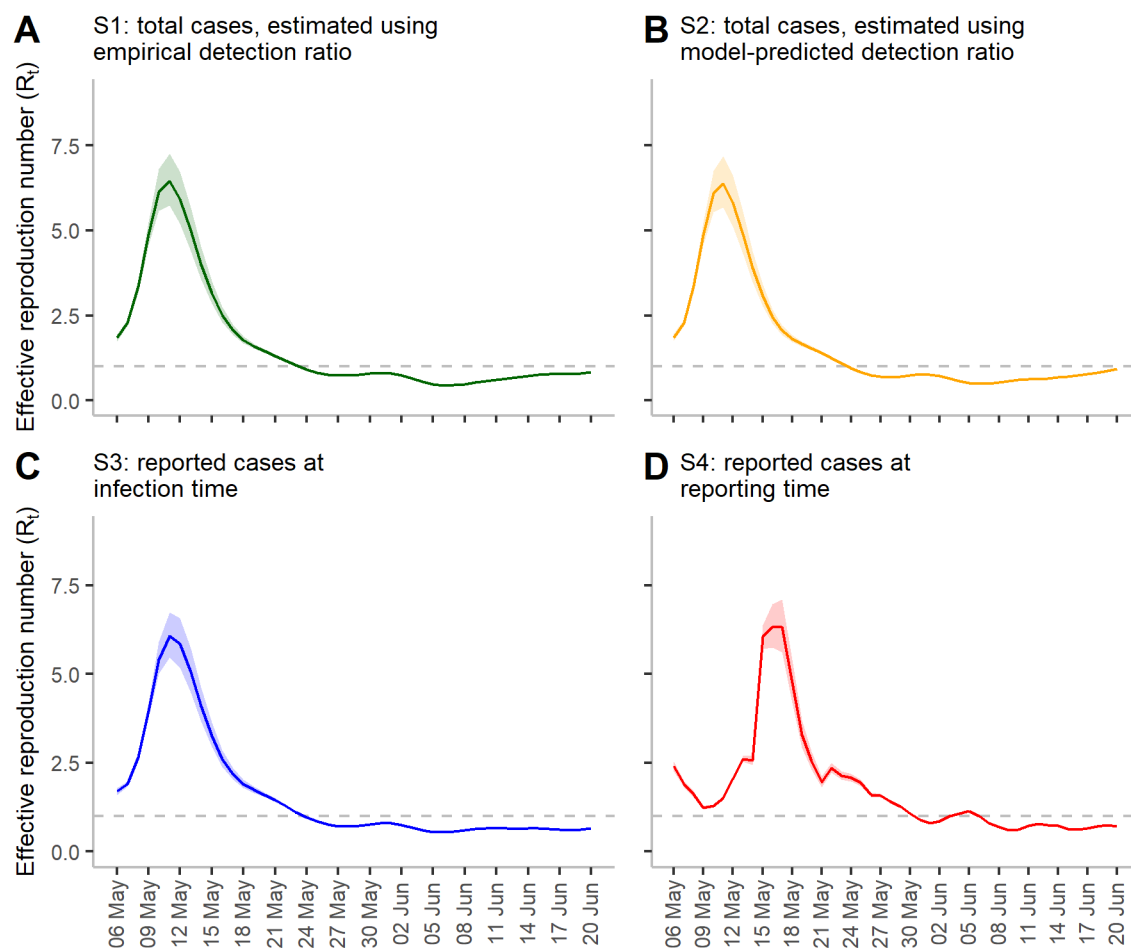
523



524

525

526 Figure S3. **(A)** Mobility index during the outbreak. The smooth line shows a 7-day moving
527 average, whereas the dots represent the observed mobility index. The vertical dashed lines
528 represent the implementation of level 2 and level 3 restrictions in May and June. Level 2
529 restrictions were started on May 11 and lasted until June 8, whereas level 3 restrictions were
530 imposed for the duration between May 19 and May 28. **(B)** Distribution of death delay. The
531 bars represent the observed frequency of delay distribution and line represents the fitted line
532 for gamma distribution with mean and standard deviation 12.7 and 5.3 days, respectively.



533

534 Figure S4. Effective reproduction number R_t during the entire period between May 6 and June
535 20. S1 and S2 refer to the numbers of total cases at infection time. S3 and S4 refer to the
536 numbers of reported cases at infection and reporting time, respectively. Smooth solid lines
537 represent the estimated mean R_t , and shaded regions show the 95% confidence intervals. The
538 dashed line depicts the cutoff value when $R_t = 1$.

539 **Supplementary tables**

540

541 Table S1. Validation of the estimates of instantaneous reproduction number using mobility
 542 adjusted regression model between May 11 and May 24 when R_t reached one. The moving
 543 average of mobility using a 7-day sliding window, centered at day 4, was considered as the
 544 predictor. AIC represents the Akaike information criterion. ΔAIC shows the differences
 545 between the smallest AIC and AIC of the i th model. We rechecked the values for an extended
 546 period until May 27, when R_t reached a minimum. In this case, R_t , estimated under scenario
 547 S1, showed the best fit of the mobility data with minimum AIC -27.93 (data is not presented
 548 in this table), whereas scenario S2 was treated as the second-best with AIC -27.20. The
 549 difference between the AIC of these two scenarios was less than one.

Date	Type of data R_t estimated from	Validation window 11 May- 24 May	
		AIC	ΔAIC
At infection time	S1: Total cases estimated using the empirical detection ratio	-27.93	0.00
	S2: Total cases estimated using the model-predicted detection ratio	-27.20	0.73
	S3: Reported cases	-21.70	6.23
At reporting time	S4: Reported cases	27.56	55.49

550